Scalable Optimal Control Allocation: Linear and Quadratic Programming Methods Applied to Active Capacitor Balancing in Modular Multilevel Converters

Grégoire Le Goff, Maurice Fadel, Marc Bodson

Scalable Optimal Control Allocation: Linear and Quadratic Programming Methods Applied to Active Capacitor Balancing in Modular Multilevel Converters

Grégoire Le Goff * **Maurice Fadel** * **Marc Bodson** **

* *LAPLACE, Université de Toulouse, CNRS, INPT, UPS, Toulouse, France (e-mail: legoff@laplace.univ-tlse.fr, fadel@laplace.univ-tlse.fr).*
** *Department of Electrical and Computer Engineering, University of Utah, Salt Lake City, Utah, USA (e-mail: bodson@eng.utah.edu)*

Abstract: The paper introduces a novel, scalable control allocation (CA) formulation for active capacitor balancing of the Modular Multilevel Converter (MMC). The formulation is obtained by introducing a converter arm model that is also scalable and accommodates an MMC with any number of phases and any number of submodules (SM). The CA algorithm involves the fast real-time minimization of an error cost function formalized as linear programming (LP) and quadratic programming (QP) problems. The real-time coding is implemented in both cases using an interior-point method. A hardware-in-the-loop (HIL) test procedure is used to demonstrate the ability of the CA to perform active capacitor voltage balancing. The influence of QP vs LP on the system behavior is also evaluated, and tracking errors using QP are found to be more evenly distributed than with LP.

Keywords: Control Allocation, Online Optimization, Fast Real-Time Optimization, Scalable Control, MMC, Capacitor Voltage Balancing, Scalable Model

1. INTRODUCTION

1.1 Control Allocation: from aeronautics to a diversification of the application fields

The control method studied in this paper is a control allocation (CA) method. The objective of such methods is to take advantage of multiple degrees of freedom of the control input in order to optimally govern the considered system. CA methods first appeared in aeronautics (Ryanski, 1983) and have undergone a large and steady development in this domain until today (Bodson, 2002; Härkegård, 2003; Frost and Bodson, 2010; Johansen and Fossen, 2013; Tohidi et al., 2017; Kolaric et al., 2020). However, these methods have spread to other domains: spacecraft, ships, automotive and land vehicles. More recently, applications have been added to power converters in electrical engineering, (Bouarfa et al., 2018, 2019; Kreiss et al., 2021) which is the subject of this article.

1.2 Objective of the research work

The objective of the research project is to develop control allocation methods for electrical systems with a large number of switches (i.e., a large number of control variables) of the Modular Multilevel Converter (MMC) type. The work proposed in this paper aims at presenting results from the exploration of this research. The control of the MMC must ensure two main objectives: the tracking of current references as well as the voltage balancing in the capacitors (Sharifabadi et al., 2016; Zama, 2017). This study focuses on the second objective, although the first one is ensured by another component to guarantee proper operation of the MMC.

1.3 Novelty of the proposed work

Since the advent of the MMC (Lesnicar and Marquardt, 2003), various methods of capacitor balancing have been studied (Zama, 2017), such as Selective Harmonic Elimination, Nearest Level Control, Frequency Mitigation, Voltage Ripple Mitigation, Natural Balancing... These methods compute in a deterministic way the control vector to be applied by making a reasonable choice of value to give to each of the control variables. However, this choice is not necessarily the best possible, because it is not the result of optimization. Processors are now powerful enough to run optimization algorithms in real time to solve control problems at increasing sampling rates (Härkegård, 2003; Petersen and Bodson, 2005, 2006; Bouarfa et al., 2018; Wei et al., 2022).

The main contribution of this paper is the use of an optimal CA method to determine the MMC control actions for active capacitor balancing. Compared to previous works, a major novelty is the scalability of the proposed method: a generalized scalable model of the MMC arms is introduced in Section 2, making possible the scalable formulation of the CA control algorithm to an MMC having any number of phases and submodules (SM) in Sections 2.2 and 3. The paper thus introduces a more general and scalable formulation than that of (Bouarfa et al., 2019), while focusing on capacitor balancing, which is a new. Finally, Section 4 reports the results of Hardware-In-the-Loop (HIL) tests of the control allocation algorithm and a detailed comparative study of the CA formulation for the linear programming (LP) versus the quadratic programming (QP). Differences between the behavior of

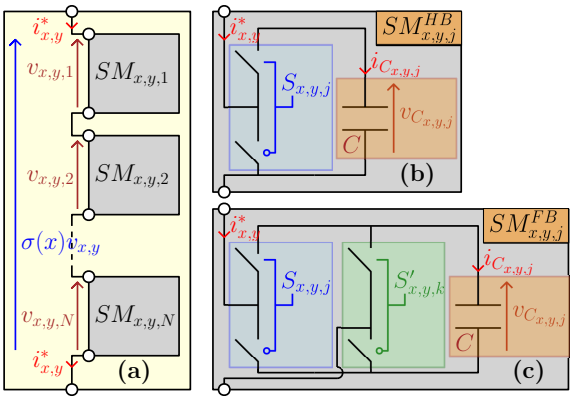

Fig. 1. (a) MMC arm $\#\{x, y\}$ out of $2m$ arms. (b) and (c) are the MMC submodules types most commonly used with (b) Half-Bridge and (c) Full-Bridge.

the system in closed loop using the two options are also discussed.

2. MODEL OF THE SYSTEM

2.1 Submodule Model

The architecture of the most common SMs (Marquardt, 2018) composing the arms of an MMC converter is shown Fig. 1 where half-bridge submodules (SM-HB) and full-bridge submodules (SM-FB) are depicted and N is the number of SMs per arm. The model neglects resistances in the system (e.g., in switches, storage components, and lines). However, these elements have very small values and improve system stability by adding damping. The small impact on the responses is also compensated through the feedback system. On Fig. 1, the cell $\#\{x, y, j\}$ is represented, that is, the j^{th} cell of the arm x of the phase y. $S_{x,y,j}$ represents the switching state of this cell and $i^*_{x,y}$ is the current flowing through the arm $\#\{x, y\}$. All capacitors in the converter have the same capacitance C and $v_{C_{x,y,j}}$ is the voltage across the cell capacitor $\#\{x, y, j\}$. A model of the cell is:

$$i_{C_{x,y,j}} = C\frac{dv_{C_{x,y,j}}}{dt} \iff i^*_{x,y}S_{x,y,j} = C\frac{dv_{C_{x,y,j}}}{dt} \quad (1.a)$$

In the case of SM-FB cells of Fig. 1 (c) with $S'_{x,y,j}$ the second switching state of the full-bridge, Kirchhoff's current law with (1.a) gives:

$$i^*_{x,y}(S_{x,y,j} - S'_{x,y,j}) = C\frac{dv_{C_{x,y,j}}}{dt} \quad (1.b)$$

Note that (1.b) is more general than (1.a) and, in order to switch from SM-FB to SM-HB, one only needs to replace $S'_{x,y,j}$ with 0. Thus, further derivations are continued for the SM-FB case.

2.2 Converter Arm Model

Let $\mathbf{v_{Cx,y}} = [v_{C_{x,y,1}} \dots v_{C_{x,y,N}}]^T$ and $\mathbf{S^e_{x,y}} = [S_{x,y,1}, S'_{x,y,1} \dots S_{x,y,N}, S'_{x,y,N}]^T$. (1.b) being true for j ranging from 1 to N yields:

$$\dot{\mathbf{v}}_{\mathbf{Cx,y}} = \frac{i^*_{x,y}}{C} L^e_{LL} \mathbf{S^e_{x,y}} \quad (2)$$

with:

$$L^e_{LL} = \begin{bmatrix} 1 & -1 & & \\ & \ddots & \ddots & \\ & & 1 & -1 \end{bmatrix} \in \mathcal{M}_{N,2N}(\mathbb{R}) \quad (3)$$

Equation (2) describes the behavior of the capacitors in a full arm of the converter in the SM-FB case.

The proposed control method will be executed at a sampling period equal to the switching period of the converter T_s. Thus, the algorithm will use an *average model* at the switching period, expressed in discrete-time. Equation (2) includes a state-control product making the state-space model nonlinear. However, the assumption is made that $i^*_{x,y}$ can be considered constant at the scale of the sampling period, because it will have a fundamental frequency equal to that of the AC network (of the order of a few tens of Hz), whereas the sampling frequency of the control will be much larger (of the order of a few kHz). With $i^*_{x,y}/C$ considered constant, the discretization by matrix exponential of the *average model* of (2) is:

$$\mathbf{v_{Cx,y}}(\mathbf{k+1}) = \mathbf{v_{Cx,y}}(\mathbf{k}) + \frac{T_s i^*_{x,y}(k)}{C} L^{x,y}_{LL} \mathbf{D^{x,y}_{LL}}(\mathbf{k}) \quad (4)$$

with $L^{x,y}_{LL}$ equal to $\mathbb{I}_N$ or L^e_{LL} according to the type of SM used, while $\mathbf{D^{x,y}_{LL}}$ is equal to $\mathbf{D_{x,y}} = [D_{x,y,1}, \dots D_{x,y,N}]^T \in \mathbb{R}^N$ or to $\mathbf{D^e_{x,y}} = [D_{x,y,1}, D'_{x,y,1}, \dots D_{x,y,N}, D'_{x,y,N}]^T \in \mathbb{R}^{2N}$ according to the SM, where $D_{x,y,j} = \langle S_{x,y,j} \rangle_{T_s}$ and $D'_{x,y,j} = \langle S'_{x,y,j} \rangle_{T_s}$ are the duty cycles of the switches. $\langle x \rangle_{\Delta t}$ is the sliding average value of x on a Δt time window. k represents the present time $t = kT_s$ and $k+1$ the next sampling time. Thus, in both the SM-HB case and the SM-FB case the model can be put into the form (4), without loss of generality.

The control to be developed will not have as unique objective to actively balance the capacitors. Indeed, this control stage is placed at the lower level in the general control architecture compared to the current control loop, so that another objective will be to ensure the tracking of the voltage reference $v^{ref}_{x,y}$ imposed by the current control loop. From Fig. 1 (a), the voltage $v_{x,y}$ expressed in the *average model* satisfies:

$$\sigma(x)v_{x,y} = \sum_{j=1}^{N} v_{x,y,j} = \sum_{j=1}^{N} v_{C_{x,y,j}} \left(D_{x,y,j} - D'_{x,y,j}\right) \quad (5)$$

with $\sigma(x) = 1$ for positive arms ($x = p$) and $\sigma(x) = -1$ for negative arms ($x = n$). Note that $\sigma(x) = 1/\sigma(x)$, so that $\sigma(x)$ can be moved to the right-hand side of (5). The state-command product in (5) makes the model nonlinear, but the voltage across the capacitors is considered constant at the scale of the sampling period for the same reasons as $i^*_{x,y}$ in (3). Equation (5) is therefore discretized as:

$$v_{x,y}(k) = \sigma(x)\ \mathbf{v_{Cx,y}}(\mathbf{k})^T\ L^{xy}_{LL}\ \mathbf{D^{x,y}_{LL}}(\mathbf{k}) \quad (6)$$

So that the active capacitor balancing control stage ensures: 1) the tracking of $v^{ref}_{x,y}$, and 2) the balancing of the capacitors by tracking of the reference $v_C{}^{ref}_{x,y}$, the control algorithm will use models (4) and (6), combined as:

$$\begin{bmatrix} \sigma(x)v_{x,y}(k) \\ \mathbf{v_{Cx,y}}(\mathbf{k+1}) - \mathbf{v_{Cx,y}}(\mathbf{k}) \end{bmatrix} = \begin{bmatrix} \mathbf{v_{Cx,y}}(\mathbf{k})^T\ L^{x,y}_{LL} \\ \dfrac{T_s i^*_{x,y}(k)}{C} L^{x,y}_{LL} \end{bmatrix} \mathbf{D^{x,y}_{LL}}(\mathbf{k}) \quad (7)$$

The duty cycles $\mathbf{D^{x,y}_{LL}}(\mathbf{k})$ of the SMs of the arm should be computed so that (8) is satisfied at any time k :

$$\begin{bmatrix} \mathbf{v_{Cx,y}}(\mathbf{k})^T\ L^{x,y}_{LL} \\ \dfrac{T_s i^*_{x,y}(k)}{C} L^{x,y}_{LL} \end{bmatrix} \mathbf{D^{x,y}_{LL}}(\mathbf{k}) = \begin{bmatrix} \sigma(x)v^{ref}_{x,y}(k) \\ \mathbf{v^{ref}_{Cx,y}}(\mathbf{k}) - \mathbf{v_{Cx,y}}(\mathbf{k}) \end{bmatrix} \quad (8)$$

with $\mathbf{v_{C_{x,y}}^{ref}}(\mathbf{k})$ the voltage vector that is desired across the capacitors at time $k+1$, that is to say the reference that is given at time k. It is thus possible to introduce the following notation for (8):

$$M_{LL}^{x,y}\ \mathbf{U_{LL}^{x,y}} = \mathbf{a_{d_{LL}}^{x,y}} \tag{9}$$

Equations (8) and (9) having been established for an arm x, y containing SMs of any type (HB or FB) and any quantity $N \in \mathbb{N}^*$, this equation embodies a voltage-level control model that is modular and scalable to an arm containing any number of SMs. Possible numbers range from 3 (Le Goff et al., 2021, 2022) to 400 (Peralta et al., 2012), or even more. Equation (9), derived by considering $i_{x,y}^*$ and $\mathbf{v_{Cx,y}}$ constant over T_s, implicitly assumes that the arms of the converter behave independently of each other. In reality they exchange currents, but this characteristic is not directly taken into account here. Since equation (9) is true $\forall x \in \{p, n\}$ and $\forall y \in \{y_1, \ldots, y_m\}$, a matrix model representing the set of MMC arms can easily be implemented by concatenating (9) for each arm: $M_{LL}\ D_{LL} = a_{d_{LL}}$. This matrix formulation adapts itself to the number of SMs, to their type, and to the number of phases, embodying a voltage-level control model that is modular and scalable to any MMC containing SM-HBs or SM-FBs.

3. CONTROL ALLOCATION FORMULATION

3.1 Control Allocation Problem

Control Allocation refers to a control method that has taken different formalisms in the literature (Bodson, 2002; Johansen and Fossen, 2013; Kolaric et al., 2020), but in general, the point of convergence of these approaches is a control problem that can be written as:

$$\{M\ \mathbf{U} = \mathbf{a_d} \mid \mathbf{U}_{min} \leq \mathbf{U} \leq \mathbf{U}_{max}\} \tag{10}$$

where $\mathbf{U} \in \mathbb{R}^{n_U}$ is the control vector that is to be computed, $\mathbf{a_d} \in \mathbb{R}^{n_a}$ is the action vector that is desired to be reached, and $M \in \mathcal{M}_{n_a,n_U}(\mathbb{R})$ is the matrix representing the effect of $\mathbf{U}$ on the system to be controlled (i.e., the effectiveness of the redundant actuators). The objective is to determine the command $\mathbf{U}$ allowing the system to reach $\mathbf{a_d}$, given constraints on the vector $\mathbf{U}$ (typically upper and lower bounds, resp. $\mathbf{U}_{max}$ and $\mathbf{U}_{min}$).

Various CA methods have emerged (Johansen and Fossen, 2013) that can be gathered into three families: 1) Model-Inversion-Based (Johansen and Fossen, 2013; Bordignon and Durham, 1995; Boskovic and Mehra, 2002), 2) Error Minimization Online (Bodson, 2002; Härkegård, 2003; Petersen and Bodson, 2006; Frost and Bodson, 2010), and 3) Error Minimization Offline (Liao et al., 2007; Tohidi et al., 2017; Kolaric et al., 2020). The second family presents the best trade-off between implementation complexity, resolution efficiency (quality of the solution with respect to (10)), and computational speed. The objective of the next two sections is to introduce a formalization of (9) adapted to this family of methods.

3.2 Formulation for Linear Programming

The objective of the control allocation is to find $\mathbf{U}$ bounded by $\mathbf{U}_{min}$ and $\mathbf{U}_{max}$ solving (10), or providing the best solution possible. A deviation variable $\mathbf{e}$ is introduced:

$$\mathbf{e} = M\ \mathbf{U} - \mathbf{a_d} \tag{11}$$

The optimization will aim to minimize an $\mathbf{e}$-dependent criterion under the constraint $\mathbf{U}_{min} \leq \mathbf{U} \leq \mathbf{U}_{max}$. In the linear programming (LP) framework, the cost function must be a linear criterion, hence the choice of $l1$-norm :

$$\begin{cases} \min\limits_{\mathbf{U},\mathbf{e}} J_{LP} = |\mathbf{e}| = \sum\limits_{i=1}^{n_a} |e_i| \\ \text{under the constraints } (u.c.) : \\ M\ \mathbf{U} - \mathbf{e} = \mathbf{a_d} \\ \mathbf{U}_{min} \leq \mathbf{U} \leq \mathbf{U}_{max},\ \ -\mathbf{e}_{max} \leq \mathbf{e} \leq \mathbf{e}_{max} \end{cases} \tag{12}$$

where $\mathbf{e}_{max}$ is some upper bound on the achievable error. Here: $\mathbf{e}_{max} = \max(abs(\mathbf{a_d}))\ [1 \ldots 1]^T \in \mathbb{R}^{n_a}$, although other ways have been used (Bodson, 2002). LP algorithms solve problems of the form (13):

$$\begin{cases} \min\limits_{\mathbf{x}} J_{LP} = \mathbf{c}^T\mathbf{x} \\ u.c. :\ A\ \mathbf{x} = \mathbf{b} \\ \qquad \mathbf{0} \leq \mathbf{x} \leq \mathbf{x}_{max} \end{cases} \tag{13}$$

To exploit the formulation (13), $\mathbf{e}$ is decomposed into $\mathbf{e} = \mathbf{e}^+ - \mathbf{e}^-$ with $\mathbf{e}^+, \mathbf{e}^- \geq 0$ and a change of variable is made on $\mathbf{U} : \mathbf{U} = \overline{\mathbf{U}} - \mathbf{U}_{min}$. Thus, (12) takes the form of (13) whose parameters are then:

$$\begin{array}{l} \mathbf{x} = \left[\overline{\mathbf{U}}\ \mathbf{e}^+\ \mathbf{e}^-\right]^T \in \mathbb{R}^{n_U+2n_a} \\ \mathbf{c}^T = [\mathbb{0}_{1,n_U}\ 1 \ldots 1\ 1 \ldots 1] \in \mathbb{R}^{n_U+2n_a} \\ A = [M\ -\mathbb{I}_{n_a}\ +\mathbb{I}_{n_a}] \in \mathcal{M}_{n_a,n_U+2n_a}(\mathbb{R}) \\ \mathbf{b} = [\mathbf{a_d} - M\ \mathbf{U}_{min}] \in \mathbb{R}^{n_a} \\ \mathbf{x}_{max} = [\mathbf{U}_{max} - \mathbf{U}_{min}\ \mathbf{e}_{max}\ \mathbf{e}_{max}] \in \mathbb{R}^{n_U+2n_a} \end{array} \tag{14}$$

It is important to note that it is possible to take into account a weighting of the control objectives represented by (10) in general, and by (8) in the case of the converter. Indeed, it is possible to multiply a line of M, and the corresponding line of $\mathbf{a_d}$, by the same factor to give them more or less importance in the cost function. With the converter for example, if one wishes to give more importance to the control objective of tracking $v_{x,y}^{ref}$ and less importance to $\mathbf{v_{C_{x,y}}^{ref}}$ tracking, (8) can be modified to:

$$\begin{bmatrix} \mathbf{v_{Cx,y}}(\mathbf{k})^T\ L_{LL}^{x,y} \\ \varepsilon_0 \dfrac{T_s i_{x,y}^*(k)}{C} L_{LL}^{x,y} \end{bmatrix} \mathbf{D_{LL}^{x,y}}(\mathbf{k}) = \begin{bmatrix} \sigma(x) v_{x,y}^{ref}(k) \\ \varepsilon_0 \left(\mathbf{v_{C_{x,y}}^{ref}}(\mathbf{k}) - \mathbf{v_{Cx,y}}(\mathbf{k})\right) \end{bmatrix} \tag{19}$$

with $\varepsilon_0 < 1$ (in this study, $\varepsilon_0 = 0.5$). Equation (19) then redefines the matrices M and $\mathbf{a_d}$ but no changes need to be made to the algorithm solving (13).

3.3 Formulation for Quadratic Programming

Interior-Point (Petersen and Bodson, 2006) and Active-Set (Härkegård, 2003) algorithms have been used to solve QP problems in real time, based on the formulation:

$$\begin{cases} \min\limits_{\mathbf{x}} J_{QP} = \dfrac{1}{2}\mathbf{x}^T H \mathbf{x} + \mathbf{c}^T\mathbf{x} + f \\ u.c. :\ A\ \mathbf{x} = \mathbf{b} \\ \qquad \mathbf{x}_{min} \leq \mathbf{x} \leq \mathbf{x}_{max} \end{cases} \tag{20}$$

Compared to (12), the use of the $l2$-norm gives:

$$\begin{cases} \min\limits_{\mathbf{U},\mathbf{e}} J_{QP} = ||\mathbf{e}||^2 = \sum\limits_{i=1}^{n_a} e_i^2 \\ u.c. :\ M\ \mathbf{U} - \mathbf{e} = \mathbf{a_d} \\ \qquad \mathbf{U}_{min} \leq \mathbf{U} \leq \mathbf{U}_{max},\ \ -\mathbf{e}_{max} \leq \mathbf{e} \leq \mathbf{e}_{max} \end{cases} \tag{21}$$

The formulation for real-time quadratic programming becomes:

$$
\begin{aligned}
&\mathbf{x} = [\mathbf{U}\ \mathbf{e}]^T \in \mathbb{R}^{n_U+n_a} \\
&H = 2\begin{bmatrix} \mathbb{O}_{n_U} & \\ & \mathbb{I}_{n_a} \end{bmatrix} \in \mathcal{M}_{n_U+n_a}(\mathbb{R}) \\
&\mathbf{c}^T = [\mathbb{O}_{1,n_U+n_a}] \in \mathbb{R}^{n_U+n_a} \qquad f = 0 \\
&A = [M\ -\mathbb{I}_{n_a}] \in \mathcal{M}_{n_a,n_U+n_a}(\mathbb{R}) \\
&\mathbf{b} = [\mathbf{a_d}] \in \mathbb{R}^{n_a} \\
&\mathbf{x}_{min} = [\mathbf{U}_{min}\ -\mathbf{e}_{max}] \in \mathbb{R}^{n_U+n_a} \\
&\mathbf{x}_{max} = [\mathbf{U}_{max}\ \mathbf{e}_{max}] \in \mathbb{R}^{n_U+n_a}
\end{aligned}
\tag{22}
$$

The online optimization solution of (12) (resp. (21)) will be performed by the Interior-Point algorithm developed by (Petersen and Bodson, 2005) (resp. (Petersen and Bodson, 2006)). Even though other optimization algorithms are available, the Interior-Point algorithm has been chosen because it handles both LP and QP, which will allow us to compare (12) and (21). Parameters for LP and QP Interior-Point algorithms are $\varepsilon_s = 10^{-4}$ and $\rho = 0.9995$. A supplementary parameter is added to force the optimization to stop in order to prevent real-time overrun problems: the maximum number of iterations of the algorithms $i_{max} = 100$. In the case of an arm of the MMC, having N SMs means: 1) having $n_U = N$ control variables (the duty cycles), 2) one control objective which is to ensure the arm voltage reference tracking, 3) N preference objectives that are to ensure the voltage balancing of the N capacitors of the arm. Thus $n_a = 1 + N$. For the case of LP, the optimization problem size is $A : (N + 1 \times 3N + 2)$ whereas for QP, the size is: $A : (N + 1 \times 2N + 1)$. This means that in the case of the simulation results shown on Fig. 4 and Fig. 5 where $N = 7$, it comes that for LP $A : (8 \times 26)$ and for QP $A : (8 \times 17)$.

As needed for further analysis of the control performances, the following definition is introduced.

Definition 1. Let $\mathbf{x} \in \mathbb{R}^n$, the extremum gap of a given vector $\mathbf{x}$ is then expressed as $\varepsilon_g(\mathbf{x}) = |max(\mathbf{x}) - min(\mathbf{x})|$. The notion of vector uniformity is then defined as follows: the smaller $\varepsilon_g(\mathbf{x})$ is, the more uniform $\mathbf{x}$ is. If $\varepsilon_g(\mathbf{x})$ is null, the distribution of $\mathbf{x}$'s components is said to be uniform.

4. HARDWARE-IN-THE-LOOP TESTS RESULTS

4.1 Test Procedure

The procedure tests the online optimization CA methods using LP and by QP methods for the control of an

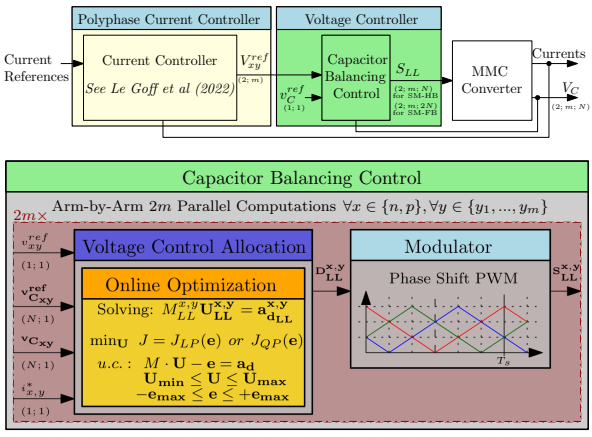

Fig. 2. MMC control architecture: (a) current control outer-loop and capacitor voltage active-balancing control inner-loop, (b) zoom on the second loop.

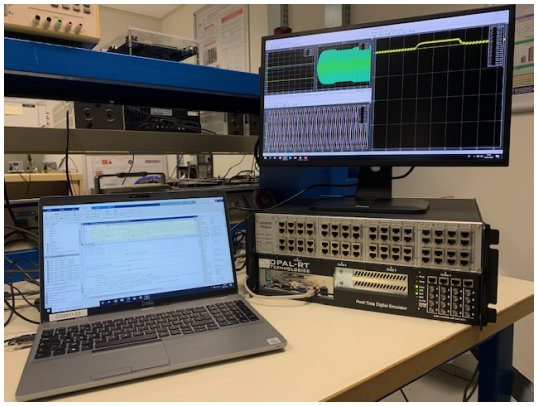

Fig. 3. Hardware-In-the-Loop test setup with the Opal-RT 5600 HIL box at the LAPLACE laboratory.

MMC. As (4) indicates, the arm currents are, together with the duty cycles, responsible for the evolution of the voltages across the capacitors. Therefore, the control of these currents is necessary in order to control the capacitor balancing. The control architecture shown on Fig. 2 (a) tests the active balancing of the capacitors with an external current control loop. This loop takes advantage of the method proposed in (Lizana et al., 2015; Le Goff et al., 2022) by developing the control from the scalable current-level model of (Le Goff et al., 2021, 2022) and controlling the currents for an MMC connected to a polyphase network. Since the focus is on the behavior of the capacitor balancing in closed-loop, the high-level current controller will maintain the currents at their nominal value while the control of capacitor voltages is under scrutiny in transient and steady-state conditions. Fig. 3 shows the setup of the HIL procedure, while hardware parameters are given in Table 1.

Table 1. HIL Test Parameters

Meaning	Symbol	Value
MMC Hardware Capacitor-Balancing Parameters		
Capacitor voltage	v_C^{nom}	200 V
Submodules per arm	N (several tests)	$3, 7, 50, 400$
Bus voltage	$V_{DC} = Nv_C^{nom}$	$N \cdot 200$ V
Capacitor capacity	C	2 mF
Switching frequency	f_s (T_s)	4 kHz (250 µs)
$v_{x,y}$ fundam. frequency	f_o (T_o)	50 Hz (20 ms)
For the remaining MMC parameters see (Le Goff et al., 2022)		
Opal-RT 5600 HIL Box Parameters		
CPU Type	–	Intel Xeon X5690
CPU Clock	–	3.46 GHz
CPU Cache / RAM	–	12 Mb / 4 Gb
Closed-Loop Simulation Parameters		
Simulation time step	T_{step}	$T_s/100 = 2.5$ µs
Simulation end time	t_{end}	$42\ T_o = 840$ ms

Figs. 4-5 show the closed-loop HIL test using control allocation. Computations were found to require less than 250 µs. Note that results are similar in all the other legs and arms of the converter, thus only results in one arm are shown. The capacitor voltage ripple is due to the AC components of the currents flowing through the MMC, which is normal. The tests show that tracking of the arm voltage references as well as the capacitor voltage balancing are successfully performed, *validating the proposed online optimization CA as a solution for the voltage control within the MMC.*

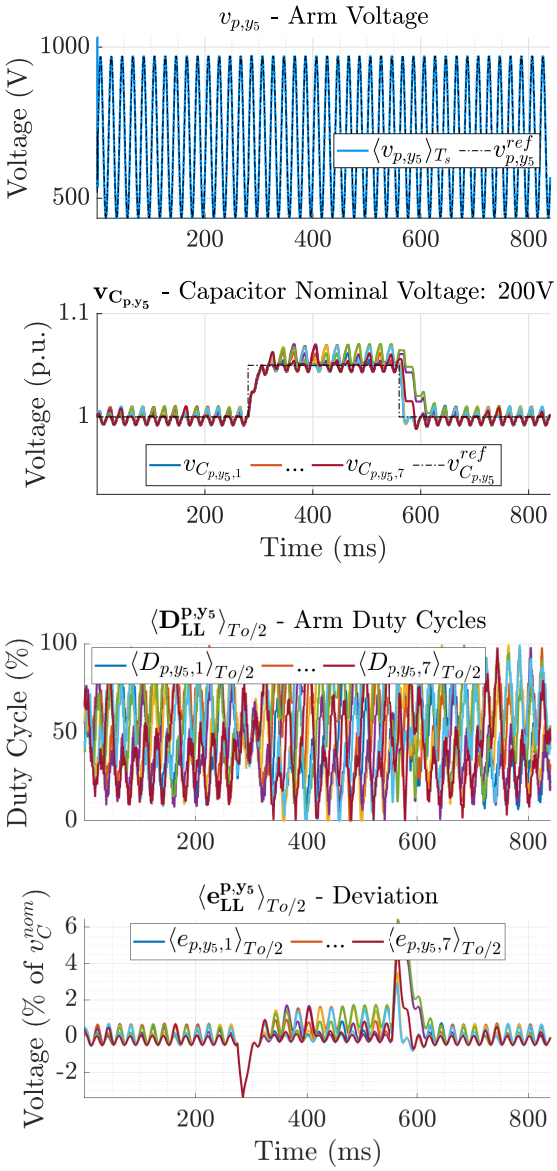

Fig. 4. Closed-loop HIL test results using LP for the 5-phase case, $N = 7$ SMs. Arm voltage, capacitor voltages, duty cycles and deviation for the upper arm $x = p$ from leg $y = y_5$.

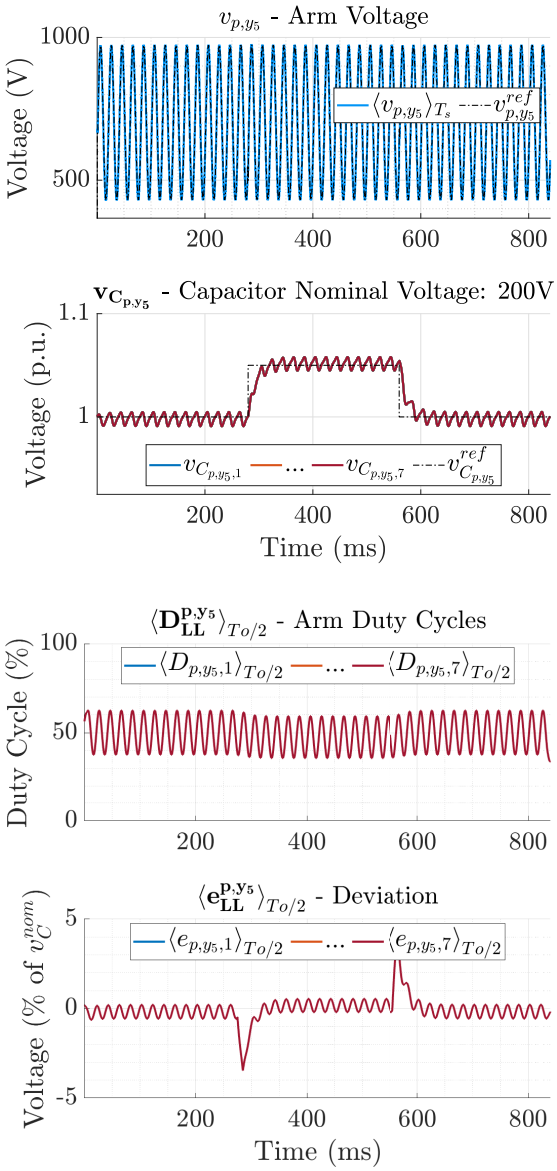

Fig. 5. Closed-loop HIL test results using QP for the 5-phase case, $N = 7$ SMs. Arm voltage, capacitor voltages, duty cycles and deviation for the upper arm $x = p$ from leg $y = y_5$.

Comparing Figs. 4 and 5, the tests show that, using QP for the MMC capacitor balancing control stage results in a more uniform distribution of the deviations e_i (according to *Definition* 1) and a more balanced use of control variables than using LP. This phenomenon was observed in the context of control allocation applied to the aerospace domain (Frost and Bodson, 2010).

The following argument is proposed to shed some light on this difference of behavior. Let $\mathbf{U(k)}$, the allocated control at time k, such that it ensured an ideal allocation: $\mathbf{e(k)} = 0$. Two neighboring situations are compared at time $k+1$. Assume that solutions $\mathbf{U_1(k+1)}$ and $\mathbf{U_2(k+1)}$ exist such $\mathbf{U_1(k+1)}$ gives a uniformly distributed deviation

$$\mathbf{e_1(k+1)} = [\delta e \dots \delta e \ \delta e \ \delta e \ \delta e \dots \delta e] \in \mathbb{R}^{n_a}, \delta e \in \mathbb{R}, \quad (23)$$

according to *Definition* 1, $\varepsilon_g(\mathbf{e_1(k+1)}) = 0$ confirms that $\mathbf{e_1(k+1)}$ is uniformly distributed. While $\mathbf{U_2(k+1)}$ leads to:

$$\mathbf{e_2(k+1)} = [\delta e \dots \delta e \ (1-\alpha)\delta e \ (1+\alpha)\delta e \ \delta e \dots \delta e] \in \mathbb{R}^{n_a} \quad (24)$$

with $\alpha \in]0;1]$ and $\varepsilon_g(\mathbf{e_2(k+1)}) = 2\ \alpha\ \delta e$, meaning that $\mathbf{U_2(k+1)}$ gives a less uniformly distributed deviation than $\mathbf{U_1(k+1)}$. The closer α is chosen to zero, the more $\mathbf{U_1(k+1)}$ and $\mathbf{U_2(k+1)}$ will be neighboring solutions. By comparing these different solutions with the two criteria, it is observed that:

$$\begin{array}{ll} J_{LP_1} = |\mathbf{e_1}| = n_a\ |\delta e| & J_{LP_2} = |\mathbf{e_2}| = n_a\ |\delta e| \\ J_{QP_1} = ||\mathbf{e_1}||^2 = n_a\ \delta e^2 & J_{QP_2} = ||\mathbf{e_2}||^2 = (n_a + 2\alpha^2)\ \delta e^2 \end{array} \quad (25)$$

Thus, $J_{LP_2} = J_{LP_1}$ and $J_{QP_2} > J_{QP_1}$. In other words, the QP will always choose the solution that balances the deviations, while the LP criterion will not.

Contrary to the LP, the QP will favor the choice of a control $\mathbf{U}$ which, through the contribution of each of the u_j to the generation of the desired control objective $\mathbf{a_d}$, will generate a gap $\mathbf{e}$ whose components e_i are balanced as long

as the u_j do not saturate. This means that all the u_j will be selected according to their weight in the contribution to the generation of $\mathbf{a_d}$, weights which are the terms of M, in order to have balanced e_i gaps. In other words, the weighted contributions of the u_j will be balanced.

In the particular case of the converter control, Figs. 4-5 show that the capacitor voltages are balanced in steady state such that $\forall i,j \in [\![1,N]\!]^2, v_{C_{x,y,i}} \simeq v_{C_{x,y,j}}$. Since the voltage reference for all the capacitors is the same, $\forall i,j \in [\![1,N]\!]^2, v^{ref}_{C_{x,y,i}} - v_{C_{x,y,i}} \simeq v^{ref}_{C_{x,y,j}} - v_{C_{x,y,j}}$ in steady state. Moreover, in the second part of the matrix M, the same coefficient $T_s i^*_{x,y}(k)/C$ weights all the remaining rows of the matrix. Through $M^{x,y}_{LL}$ (9) it is thus found that the converter has control variables that have very close weighting in contributing to the achievement of the control objective $\mathbf{a^{x,y}_{d_{LL}}}$. Having approximately the same weighting, these degrees of freedom, which are the duty cycles, will be used in a balanced way by the QP, contrary to the case of resolution by LP, as shown by the HIL test in Figs. 4-5.

5. CONCLUSION

A scalable control-oriented model of the MMC arms was derived. The scalable model was then used to develop a scalable control allocation which is the main novelty of the paper: it is now possible to develop efficient control laws to master active balancing in a MMC of any size using fast real-time optimization, in this case it took less than 250 µs.

Both LP and QP formulations were shown to be applicable, but it was found that the use of QP will choose a control $\mathbf{U}$ so that its contribution to the generation of the control objective $\mathbf{a_d}$ uniformly distributes the deviations of the errors $\mathbf{e}$.

REFERENCES

Bodson, M. (2002). Evaluation of optimization methods for control allocation. *Journal of Guidance, Control, and Dynamics*, 25(4), 703–711.

Bordignon, K. and Durham, W. (1995). Null-space augmented solutions to constrained control allocation problems. In *Guidance, Navigation, and Control Conference*. American Institute of Aeronautics and Astronautics.

Boskovic, J. and Mehra, R. (2002). Control allocation in overactuated aircraft under position and rate limiting. In *Proceedings of the 2002 American Control Conference*, volume 1, 791–796 vol.1.

Bouarfa, A., Bodson, M., and Fadel, M. (2018). An optimization formulation of converter control and its general solution for the four-Leg two-Level inverter. *IEEE Transactions on Control Systems Technology*, 26(5), 1901–1908.

Bouarfa, A., Fadel, M., and Bodson, M. (2019). Optimization method based on simplex algorithm for current control of modular multilevel converters. In *2019 IEEE International Conference on Industrial Technology (ICIT)*, 1220–1225.

Frost, S.A. and Bodson, M. (2010). Resource balancing control allocation. In *Proceedings of the 2010 American Control Conference*, 1326–1331.

Härkegård, O. (2003). *Backstepping and control allocation with applications to flight control*. Univ, Linköping.

Johansen, T.A. and Fossen, T.I. (2013). Control allocation—A survey. *Automatica*, 49(5), 1087–1103.

Kolaric, P., Lopez, V.G., and Lewis, F.L. (2020). Optimal dynamic control allocation with guaranteed constraints and online reinforcement learning. *Automatica*, 122(109265).

Kreiss, J., Bodson, M., Delpoux, R., Gauthier, J.Y., Trégouët, J.F., and Lin-Shi, X. (2021). Optimal control allocation for the parallel interconnection of buck converters. *Control Engineering Practice*, 109.

Le Goff, G., Fadel, M., and Bodson, M. (2022). Scalable control-oriented model of the modular multilevel converter for polyphase systems. *IEEE Transactions on Industry Applications*.

Le Goff, G., Fadel, M., and Bodson, M. (2021). Modular polyphased full order current state-space model of the modular multilevel converter. In *2021 IEEE 19th International Power Electronics and Motion Control Conference (PEMC)*, 132–139.

Lesnicar, A. and Marquardt, R. (2003). An innovative modular multilevel converter topology suitable for a wide power range. In *2003 IEEE Bologna Power Tech Conference Proceedings*, volume 3.

Liao, F., Lum, K., Wang, J.L., and Benosman, M. (2007). Constrained nonlinear finite-time control allocation. In *2007 American Control Conference*, 3801–3806.

Lizana, R., Perez, M.A., Arancibia, D., Espinoza, J.R., and Rodriguez, J. (2015). Decoupled current model and control of modular multilevel converters. *IEEE Transactions on Industrial Electronics*, 62(9), 5382–5392.

Marquardt, R. (2018). Modular multilevel converters: state of the art and future progress. *IEEE Power Electronics Magazine*, 5(4), 24–31.

Peralta, J., Saad, H., Dennetiere, S., Mahseredjian, J., and Nguefeu, S. (2012). Detailed and Averaged Models for a 401-Level MMC–HVDC System. *IEEE Transactions on Power Delivery*, 27(3), 1501–1508.

Petersen, J.A.M. and Bodson, M. (2006). Constrained quadratic programming techniques for control allocation. *IEEE Transactions on Control Systems Technology*, 14(1), 91–98.

Petersen, J.A. and Bodson, M. (2005). Interior-Point Algorithms for Control Allocation. *Journal of Guidance, Control, and Dynamics*, 28(3), 471–480.

Ryanski, E.G. (1983). Experimental experience at Calspan. In *Restructurable Controls*, 99–114. Nasa Conference Publication 2277.

Sharifabadi, K., Harnefors, L., Nee, H.P., Norrga, S., and Teodorescu, R. (2016). Dynamics and control. In *Design, control, and application of modular multilevel converters for HVDC transmission systems*, 133–213. IEEE.

Tohidi, S.S., Yildiz, Y., and Kolmanovsky, I. (2017). Adaptive control allocation for over-actuated systems with actuator saturation. *IFAC-PapersOnLine*, 50(1), 5492–5497.

Wei, H., Fan, L., Ai, Q., Zhao, W., Huang, T., and Zhang, Y. (2022). Optimal energy allocation strategy for electric vehicles based on the real-time model predictive control technology. *Sustainable Energy Technologies and Assessments*, 50.

Zama, M. (2017). *Modeling and control of modular multilevel converters (MMCs) for HVDC applications*. Ph.D. Thesis, Communauté Université Grenoble Alpes.